
OUTPUT RANGE ANALYSIS FOR DEEP NEURAL NETWORKS BASED ON SIMULATED ANNEALING PROCESSES

Helder Rojas

Department of Mathematics
Imperial College London
London, United Kingdom
h.rojas-molina23@imperial.ac.uk

Nilton Rojas

Escuela Profesional de Ciencias de la Computación
Universidad Nacional de Ingeniería
Lima, Perú
nrojasv@uni.pe

Espinoza J. B.

Escuela Profesional de Ingeniería Estadística
Universidad Nacional de Ingeniería
Lima, Perú
jespinozas@uni.edu.pe

Luis Huamanchumo

Escuela Profesional de Ingeniería Estadística
Universidad Nacional de Ingeniería
Lima, Perú
lhuamanchumo@uni.edu.pe

July 4, 2024

ABSTRACT

This paper tackles the challenging problem of output range estimation for Deep Neural Networks (DNNs), introducing a novel algorithm based on Simulated Annealing (SA). Our approach addresses the lack of local geometric information and high non-linearity in DNNs, making it versatile across various architectures, especially Residual Neural Networks (ResNets). We present a straightforward, implementation-friendly algorithm that avoids restrictive assumptions about network architecture. Through theoretical analysis and experimental evaluations, including tests on the Ackley function, we demonstrate our algorithm's effectiveness in navigating complex, non-convex surfaces and accurately estimating DNN output ranges. Furthermore, the Python codes of this experimental evaluation that support our results are available in our GitHub repository*.

Keywords Deep Neural Networks, Simulated Annealing, Output Range Estimation, Residual Neural Networks, Global Optimization, Cyber-Physical Systems, Non-Convex Optimization

1 Introduction

Unquestionably, in recent decades, Deep Neural Networks (DNNs) have been by far the most widely used tools to perform complex machine learning tasks. More recently, DNNs have been used in cyber-physical systems critical to public security and integrity; such as autonomous vehicle driving and air traffic systems. Therefore, it is of pressing interest to implement security verification systems for DNNs. One of the objectives in this line of interest is the verification of the maximum and minimum values assumed by a DNN, an objective commonly known as the range estimation problem, see Dutta et al. [2018], Wang et al. [2018]. However, the relationships established between the inputs and outputs of a DNN are highly non-linear and complex, difficult to understand with existing tools today. Due to this inability, DNNs are commonly referred to as black boxes. This nature of DNN makes the range estimation problem particularly challenging, because there is no geometric information about the response surface generated by a DNN. For example, if local geometric information about the generated surface were obtained, such as the gradient vector and the Hessian matrix at each point, the problem could be addressed with conventional nonlinear programming techniques. However, in a DNN it is only possible to obtain point information about the estimated response, without any local knowledge around that point. These facts, added to the high non-linearity of a DNN, make the range estimation problem

*<https://github.com/Nicerova7/output-range-analysis-for-deep-neural-networks-with-simulated-annealing>

non-trivial. Recently, various methodologies have been proposed for the analysis of the output range of DNNs, see for example Dutta et al. [2018], Wang et al. [2018], Tran et al. [2020], Huang et al. [2020], Liu et al. [2021]. However, these methodologies make restrictive assumptions about the network architecture which limits the use and application of these methodologies. In this paper, based on global optimization techniques, in particular Simulated Annealing, we present a simple algorithm, which contemplates the lack of local geometric information of the surfaces generated by DNNs, easy to implement and use, and that solves the range estimation problem for a wide spectrum of neural networks in general.

Outline. In Section 2 we make a mathematical description of a very particular family of deep neural networks called Residual Networks. Although our methodology works for any particular family, we focus on these neural networks given their relevance in applications and for illustrative purposes of the use of our algorithm. In Section 3 we specifically define the output range analysis problem for neural networks, mentioning its characteristics, limitations and challenges. In Section 4 we develop an exhaustive treatment of Simulated Annealing for limited domains, adapting its properties and guaranteeing its results for our purposes. In Section 5, from the above, we derive an algorithm to solve the output range analysis problem. Finally, in Section 6 we present a part of the experimental evaluations that we have executed to numerically guarantee our results and the performance of our proposed algorithm.

2 Residual Neural Networks

As already mentioned before, although our algorithm works for a wide spectrum of neural networks in general, we focus on Residual Neural Networks given their relevance in applications and for illustrative purposes of the use of our algorithm. The Residual Networks (or ResNets) were introduced in He et al. [2016], for which in this chapter we show a mathematical description. Let $x \in \mathbb{R}^d$ denote the inputs and $y \in \mathbb{R}$ be the output in a supervised learning problem. In this learning context, the objective is the approximation of a function $f : x \in \mathbb{R}^d \mapsto y \in \mathbb{R}$ using a ResNet, which we denote as \mathcal{F} . The basic unitary components of an ResNet are called neurons, which are organized in a consecutive number of layers that are linked through nonlinear functions. To obtain a mathematical description of the operations carried out within a ResNet, we define some notations. We consider a network with a source layer, a output layer and L hidden layers, where the l -th layer contains H_l neurons (l -th layer width), for $l = 0, \dots, L + 1$. Note that $H_0 = d$ and $H_{L+1} = 1$, corresponding to the feature inputs and target outputs respectively. We denote the output vector of the l -th layer by $x^{(l)} \in \mathbb{R}^{H_l}$ which corresponds to the input of the next layer. We set $x^{(0)} = x \in \mathbb{R}^d$ and $x^{(L+1)} = y \in \mathbb{R}$. For $l = 1, \dots, L$, the i -th neuron performs an affine transformation on that layers input $x^{(l-1)}$ followed by a non-linear transformation

$$x_i^{(l)} = \sigma \left(\sum_{j=1}^{H_{l-1}} W_{ij} x_j^{(l-1)} + b_i^{(l)} \right) + x_i^{(l-1)}, \quad 1 \leq i \leq H_l, \quad (1)$$

where W_{ij} and $b_i^{(l)}$ are respectively known as the weights and bias associated with i -th neuron of layer l , while the function $\sigma(\cdot)$ is known as the activation function.

Definition 1 (ResNet). Let $W^{(l)} = [W_{ij}^{(l)}] \in \mathbb{R}^{H_{l-1} \times H_l}$ be the weight matrix and $b^{(l)} = [b_i^{(l)}] \in \mathbb{R}^{H_l}$ be the bias vector for layer l , then the operations within each layer are described by

$$x^{(l)} = \sigma \left(\mathcal{A}^{(l)}(x^{(l-1)}) \right) + x^{(l-1)}, \quad \mathcal{A}^{(l)}(x^{(l-1)}) = W^{(l)}x^{(l-1)} + b^{(l)}, \quad (2)$$

where σ acts component-wise; that is, $\sigma(x_1, \dots, x_d) := (\sigma(x_1), \dots, \sigma(x_d))$. Thus, a ResNet with L hidden layers $\mathcal{F} : \mathbb{R}^d \rightarrow \mathbb{R}$ is mathematically defined as

$$\mathcal{F}(x) := \mathcal{A}^{(L+1)} \circ \sigma \circ \mathcal{A}^{(L)} \circ \sigma \circ \mathcal{A}^{(L-1)} \circ \dots \circ \sigma \circ \mathcal{A}^{(1)}(x). \quad (3)$$

Although the activation function can, in principle, be chosen arbitrarily, there are three functions that have particularly proven to be useful in various applications; ReLU, Sigmoid and Tanh, see LeCun et al. [2015], Goodfellow et al. [2016].

The parameters of the network is all the weights and biases $\{W^{(l)}, b^{(l)}\}_{l=1}^{L+1} \in \mathbb{R}^{N_p}$, where $N_p = \sum_{l=1}^{L+1} (H_{l-1} + 1)H_l$ is the total number of parameters.

3 Output Range Analysis Problem

In the rest of this paper, we consider a ResNet \mathcal{F} with inputs $x \in \mathbb{R}^d$ and output $y \in \mathbb{R}$ as defined (3). We assume that the network parameters of the neural network were optimally estimated following standard training procedures such as those shown in Bishop [2006], Murphy [2012].

Definition 2 (Range Estimation Problem). The problem is defined as follows:

- ◇ INPUTS: : Neural network, for example a ResNet \mathcal{F} , and input constraints $Ax \leq b$ which generates a feasible set E , i.e., $E = \{x \in \mathbb{R}^d : Ax \leq b\}$.
- ◇ OUTPUT: An interval $[\mathcal{F}_{min}, \mathcal{F}_{max}]$ such that $\mathcal{F}(x) \in [\mathcal{F}_{min}, \mathcal{F}_{max}]$, i.e., $[\mathcal{F}_{min}, \mathcal{F}_{max}]$ contains the range of \mathcal{F} over inputs $x \in E$. Moreover, the optimal points $\{x_{min}, x_{max}\} \in E$ such that $\mathcal{F}(x_{min}) = \mathcal{F}_{min}$ and $\mathcal{F}(x_{max}) = \mathcal{F}_{max}$.

Remark 3. Due to the applications, we focus just on hypercubes of \mathbb{R}^d as feasible set, that is; sets of the type $E = [l_1, u_1] \times \cdots \times [l_d, u_d] \subset \mathbb{R}^d$, where $[l_j, u_j]$ are intervals in \mathbb{R} .

As mentioned above, this problem is particularly challenging given that there is generally almost total ignorance about the surfaces generated by deep neural networks. That is, there is no information on the functional form of the mapping \mathcal{F} . Therefore, there is no local geometric information such as the local slopes and curvatures of these surfaces, making the use of traditional nonlinear programming methodologies impossible. Furthermore, the surfaces generated by this type of neural networks are strictly non-convex, with many crazy minima, therefore it requires thinking about global optimization methods, methods such as Simulated Annealing.

4 Simulated Annealing with Boundary Conditions

Our range estimation problem can be summarized in an optimization problem of the form

$$\min_{x \in E} \mathcal{F}, \quad (4)$$

where \mathcal{F} is a ResNet and E is a hypercubes of \mathbb{R}^d , which we denote by the pair (\mathcal{F}, E) . The main problem now is to find a point $x_{min} \in E$ such that $\mathcal{F}(x_{min})$ is global minimal on E . The $\max_{x \in E} \mathcal{F}$ is equivalent to $\min_{x \in E} -\mathcal{F}$, which is why we can, without loss of generality, only talk about ‘‘Minimization’’ throughout this paper. We denote by $M_{\mathcal{F}} = \{x_{min} \in E : \mathcal{F}(x_{min}) \leq \mathcal{F}(x), \text{ for all } x \in E\}$ the minimum set of \mathcal{F} . From Equation (3), we know that \mathcal{F} is a continuous function, and added to the fact that E is a compact set, we know that $M_{\mathcal{F}}$ is a non-empty set. For simplicity in notation we set $\mathcal{F}_{min} = \mathcal{F}(x_{min})$.

Definition 4 (Reflection). Let $E = [l_1, u_1] \times \cdots \times [l_d, u_d] \subset \mathbb{R}^d$, where $[l_j, u_j]$ are intervals in \mathbb{R} . We denote by $\mathcal{R} : \mathbb{R}^d \rightarrow E$, the different combinations of the reflections on E , that is, $\mathcal{R}(y) = (\mathcal{R}(y_1), \dots, \mathcal{R}(y_d))$, where

$$\mathcal{R}(y_j) = y_j \mathbb{1}_{(l_j, u_j)}(y_j) + (u_j - |y_j - u_j|) \mathbb{1}_{[u_j, +\infty)}(y_j) + (l_j + |l_j - y_j|) \mathbb{1}_{(-\infty, l_j]}(y_j). \quad (5)$$

Definition 5 (Generating Distribution). We say that Q is a generating distribution with Gaussian density function $\rho : E \times \mathbb{R}^d \rightarrow \mathbb{R}^+$ and with reflective boundary conditions on E , if Q is defined as

$$Q(x, B) := \int_{\{y \in \mathbb{R}^d : \mathcal{R}(y) \in B\}} \rho(x, y) dy, \quad (6)$$

where $B \subset \mathfrak{B} = \mathfrak{B}(E)$, and

$$\rho(x, y) = \frac{1}{(2\pi\sigma)^{d/2}} \exp\left(-\frac{\|x - y\|^2}{2\sigma}\right) \quad (7)$$

for $x \in E, y \in \mathbb{R}^d$ and $\sigma > 0$.

Definition 6 (Acceptance Probability). Given \mathcal{F} and a number $T > 0$, the acceptance probability $q_T : E \times E \rightarrow \mathbb{R}^+$ is defined as

$$q_T(x, y) = e^{\frac{1}{T} \min\{0, \mathcal{F}(x) - \mathcal{F}(y)\}}. \quad (8)$$

Here T is called temperature parameter.

Definition 7 (Simulated Annealing Process). Let (\mathcal{F}, E) be a global minimization problem, $(Q_i)_{i \in \mathbb{N}}$ be a sequence of generating distributions with reflective boundary conditions, $\{T_i\}_{i \in \mathbb{N}} \downarrow 0$ be a sequence of temperature parameters, and $(q_{T_i})_{i \in \mathbb{N}}$ be a sequence of acceptance probabilities. A simulated annealing process with reflective boundary conditions on E is the non-homogeneous Markov process $(X_i)_{i \in \mathbb{N}}$, defined on a probability space $(\Omega, \mathcal{A}, \mathbb{P})$, with state-space (E, \mathfrak{B}) and transition kernel $(P_i)_{i \in \mathbb{N}}$ defined by

$$P_i(x, B) = \begin{cases} \int_B Q_i(x, dy) q_{T_i}(x, y) dy & \text{for } x \notin B, \\ \int_B Q_i(x, dy) q_{T_i}(x, y) dy + \left(1 - \int_E Q_i(x, dy) q_{T_i}(x, y) dy\right) & \text{for } x \in B, \end{cases} \quad (9)$$

where $x \in E$ and $B \subset \mathfrak{B}$.

Given the transition kernel in (9), we defined the distributions of Markov process $(X_i)_{i \in \mathbb{N}}$ as $\mu_i(dx) := \mathbb{P}(X_i \in dx)$. Consequently, we have that $\mu_i = \mu_{i-1}P_i$ for $i \geq 1$, where μ_0 is an arbitrary initialization distribution on E .

Theorem 8. *Given the minimization problem (\mathcal{F}, E) , let $(X_i)_{i \in \mathbb{N}}$ a simulated annealing process with reflective boundary conditions on E . Then, for each $i \in \mathbb{N}$, the operator P_i has the equilibrium distribution π_i given by*

$$\pi_i(y) = C_i \exp\left(-\frac{\mathcal{F}(y) - \mathcal{F}_{\min}}{T_i}\right), \quad (10)$$

where C_i is the normalization constant and $\mathcal{F}_{\min} \in M_{\mathcal{F}}$. Moreover, if we set $T_i = T_0 \delta^i$, for some $|\delta| < 1$ and T_0 arbitrary, then we have that

$$\lim_{i \rightarrow \infty} \|\mu_i - \pi_i\|_{TV} = 0, \quad (11)$$

where $\|\cdot\|_{TV}$ is the total variation norm.

Proof. By construction, Q is symmetric, that is

$$\int_B Q(x, dy) = \int_B Q(y, dx), \quad (12)$$

for $B \subset \mathfrak{B}$. Furthermore, \mathcal{F} is a continuous function, and added to the fact that E is a compact set, then $M_{\mathcal{F}}$ is a non-empty set and $\mathcal{F} : E \rightarrow \mathbb{R}$ is uniform continuous. Given these facts, the results in (10) and (11) are direct applications of Theorem 5.1 and Theorem 6.5 in Haario and Saksman [1991]. \square

Corollary 9. *Suppose that the conditions of Theorem 8 are fulfilled, then*

$$\mathcal{F}(X_i) \rightarrow \mathcal{F}_{\min} \quad \text{as } i \rightarrow \infty \quad \text{in probability}, \quad (13)$$

for some $\mathcal{F}_{\min} \in M_{\mathcal{F}}$.

Proof. The proof is a slight modification of Corollary 5.4 in Haario and Saksman [1991]. \square

5 Algorithm Derivation

From Theorem 8 and its Corollary 9, a simple algorithm can easily be derived to solve the range estimation problem (\mathcal{F}, E) . The main idea is to generate a Markov process $(X_i)_{i \in \mathbb{N}}$ taking values on E , as described in Definition 7, for which its initial state is selected using an arbitrary measure μ_0 . The following states of the Markov process are selected according to two stages; In the first stage, a new state generated by Q is proposed, and subsequently in the second stage, it is decided to accept or reject that new state according to the probability of acceptance q . If the proposed state is outside the domain E we use reflection \mathcal{R} to exchange it for another equally probable state that is inside the domain E . It is important to note that the generation of new proposed states using Q is done through ρ . Both stages, proposing and accepting new states, are executed repeatedly N times for each temperature level T . Theorem 8 guarantees that if we execute this two-stage local recursive process the Markov process $(X_i)_{i \in \mathbb{N}}$ will converge towards the minimal state corresponding to the value \mathcal{F}_{\min} , this occurs for each set temperature level. Finally, Corollary 9 guarantees that if we execute the stages described above for a sequence of temperatures $\{T_i\}_{i \in \mathbb{N}}$ that slowly decreases towards zero, then the Markov process $(X_i)_{i \in \mathbb{N}}$ will converge to the minimal state corresponding to the global minimum that solves our estimation problem. We summarize the entire procedure described above in pseudocode format in Algorithm 1. In addition, we provide a Python code that is available in <https://github.com/Nicerova7/output-range-analysis-for-deep-neural-networks-with-simulated-annealing>.

6 Experimental Evaluation

To illustrate the use and operation of our algorithm we are going to use the Ackley function. In mathematical optimization, the Ackley function is a non-convex function, with many local minima, which is often used as a performance test problem for optimization algorithms. This function on a 2-dimensional domain it is defined by

$$f(x_1, x_2) = -20 \exp\left(-0.2\sqrt{0.5(x_1^2 + x_2^2)}\right) - \exp(0.5(\cos 2\pi x_1 + \cos 2\pi x_2)) + e + 20, \quad (14)$$

for which its global minimum point is $f(0, 0) = 0$, see Figure 6.1. In this case we are going to assume that $E = [-4, 4] \times [-4, 4]$. Furthermore, suppose we want to estimate the function (14) using only a discretized sample of

Algorithm 1 Minimum Output Search for a Deep Neural Network

Input: The minimization problem (\mathcal{F}, E)
Initialize $i \leftarrow 0, x \sim \mu_0, T_0 \leftarrow T_{\max}$ and $\mathcal{F}_{\min} \leftarrow \mathcal{F}(x)$
while $T_i > T_{\min}$ **do**
 for $k = 1$ to N **do**
 Generate $y \sim \rho(x, y)$
 Reflect $y \leftarrow \mathcal{R}(y)$
 Set $\Delta\mathcal{F} \leftarrow \mathcal{F}(y) - \mathcal{F}(x)$
 if $\Delta\mathcal{F} < 0$ **then**
 $q(x, y) = 1.0$
 else
 $q(x, y) = \min \left\{ 1, e^{-\frac{\Delta\mathcal{F}}{T_i}} \right\}$
 end if
 Sample $U \sim \text{Unif}(0, 1)$
 if $U \leq q(x, y)$ **then**
 Update $x \leftarrow y$
 end if
 if $\mathcal{F}(x) < \mathcal{F}_{\min}$ **then**
 $\mathcal{F}_{\min} \leftarrow \mathcal{F}(x)$
 end if
 end for
 Update $T_i = T_{i-1} \delta^i$
 Update $i \leftarrow i + 1$
end while
Output: \mathcal{F}_{\min}

points $\mathcal{D} = \{(x_{1i}, x_{2i}, f_i)\}_{i=1}^m \subset E$. To this end, we use a ResNet as described in Chapter 2, with $L = 5$ and $H_l = 10$ for $l = 2, \dots, 5$. The fit generated by these ResNet is quite good, the surface generated by the neural network maintains all the properties of the original function, including its non-convex nature and the existence of many local minima, See left side of Figure 6.2.

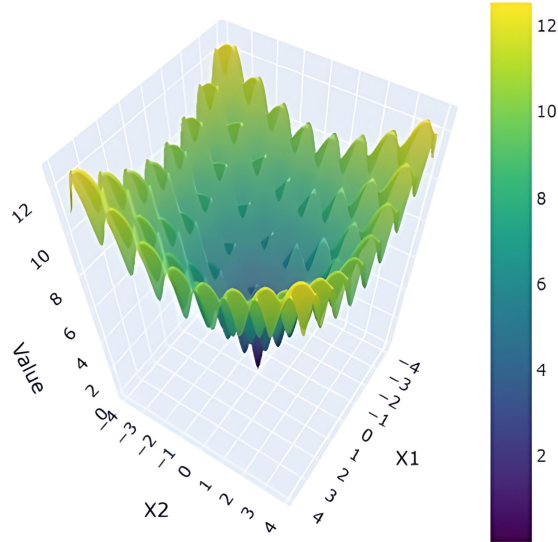


Figure 6.1: Ackley function of two variables

The fact that the generated surface consists of too many local minima constitutes a suitable scenario where our methodology shows its greatest strength. Let us remember that when working with deep neural networks, this scenario is quite recurrent due to the high non-linearity and flexibility of the relationships established by this type of neural

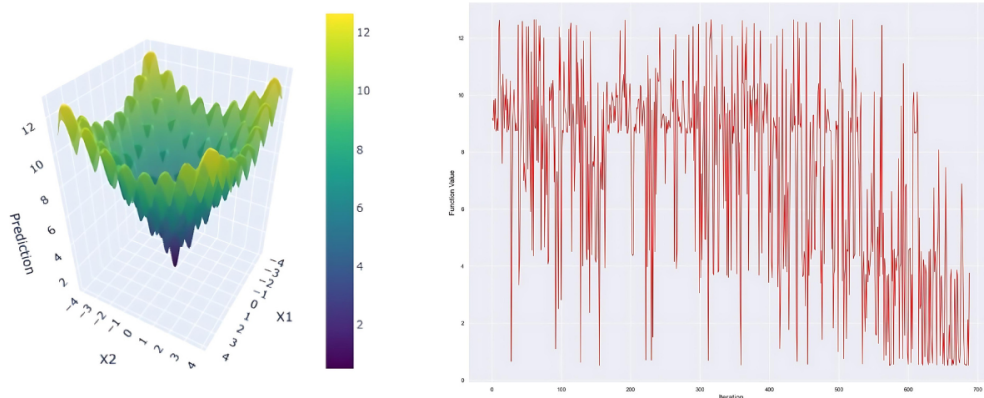


Figure 6.2: Left: Surface generated by the ResNet $(E, \mathcal{F}(E))$. Right:

networks. After training the ResNet \mathcal{F} , our main objective is to find the global minimum on the surface generated with the neural network within the domain E , denoted as $(E, \mathcal{F}(E))$. To this end, we apply our Algorithm 1 to this case. On the right side of Figure 6.2 we present the evolution of the values assumed by the Markov process generated through the algorithm. On the right side of Figure 6.2 we present the evolution of the values assumed by the Markov process generated through the algorithm. We note the reasonably fast convergence towards the global minimum $\mathcal{F}_{\min} = 0$. While it is true that there are fluctuations around the trajectory towards convergence, this is due to the highly fluctuating nature of the generated surface $(E, \mathcal{F}(E))$, but there is also a clear and consistent trend towards the global minimum 0. The Python codes of this experimental evaluation are available in <https://github.com/Nicerova7/output-range-analysis-for-deep-neural-networks-with-simulated-annealing>.

7 Conclusions

In this paper, we presented a novel approach to the output range analysis problem for Deep Neural Networks (DNNs) by employing Simulated Annealing (SA). Our methodology was specifically designed to handle the lack of local geometric information and the high non-linearity typical of DNNs. Through detailed theoretical analysis and extensive experimental evaluations, we demonstrated the effectiveness of our algorithm across a wide spectrum of neural networks, with a particular focus on Residual Networks (ResNets) due to their prominence in applications.

We began by mathematically describing ResNets and defining the output range analysis problem, highlighting the challenges posed by the complex and non-linear nature of DNN response surfaces. We then adapted the SA algorithm to this context, ensuring it could work within the bounded domains typical of DNN inputs.

References

- Bishop, C. M. (2006). *Pattern recognition and machine learning*. Springer google schola.
- Dutta, S., Jha, S., Sankaranarayanan, S., & Tiwari, A. (2018). Output range analysis for deep feedforward neural networks. In *NASA Formal Methods Symposium*, pages 121–138. Springer.
- Goodfellow, I., Bengio, Y., & Courville, A. (2016). *Deep learning*. MIT press.
- Haario, H. & Saksman, E. (1991). Simulated annealing process in general state space. *Advances in Applied Probability*, 23(4):866–893.
- Hadash, G., Kermany, E., Carmeli, B., Lavi, O., Kour, G., & Jacovi, A. (2018). Estimate and replace: A novel approach to integrating deep neural networks with existing applications. *arXiv preprint arXiv:1804.09028*.
- He, K., Zhang, X., Ren, S., & Sun, J. (2016). Deep residual learning for image recognition. In *Proceedings of the IEEE conference on computer vision and pattern recognition*, pages 770–778.
- Huang, C., Fan, J., Chen, X., Li, W., & Zhu, Q. (2020). Algorithms for verifying deep neural networks. *IEEE Transactions on Computer-Aided Design of Integrated Circuits and Systems*, 39(11):3323–3335.
- Kour, G. & Saabne, R. (2014a). Fast classification of handwritten on-line arabic characters. In *Soft Computing and Pattern Recognition (SoCPaR), 2014 6th International Conference of*, pages 312–318. IEEE.

- Kour, G. & Saabne, R. (2014b). Real-time segmentation of on-line handwritten arabic script. In *Frontiers in Handwriting Recognition (ICFHR), 2014 14th International Conference on*, pages 417–422. IEEE.
- LeCun, Y., Bengio, Y., & Hinton, G. (2015). Deep learning. *Nature*, 521(7553):436–444.
- Liu, C., Arnon, T., Lazarus, C., Strong, C., Barrett, C., Kochenderfer, M. J., et al. (2021). Algorithms for verifying deep neural networks. *Foundations and Trends® in Optimization*, 4(3-4):244–404.
- Murphy, K. P. (2012). *Machine learning: a probabilistic perspective*. MIT press.
- Tran, H.-D., Yang, X., Manzananas Lopez, D., Musau, P., Nguyen, L. V., Xiang, W., Bak, S., & Johnson, T. T. (2020). Nnv: The neural network verification tool for deep neural networks and learning-enabled cyber-physical systems. In *International Conference on Computer Aided Verification*, pages 3–17. Springer.
- Wang, S., Pei, K., Whitehouse, J., Yang, J., & Jana, S. (2018). Formal security analysis of neural networks using symbolic intervals. In *27th USENIX Security Symposium (USENIX Security 18)*, pages 1599–1614.